

# 1 Low pH Concrete for Use in the US High-Level Waste Repository: Part I Overview

Leslie R. Dole and Catherine H. Mattus  
Nuclear Science Technology Division of Oak Ridge National Laboratory

## 1.1 Introduction

The current baseline plan for the Yucca Mountain (YM) repository project (YMP) uses steel structures to stabilize the disposal drifts that are collectively over 65 kilometers in length (Figure 1-1). However using cementitious materials and application techniques, the potential exists to reduce the underground construction cost by 100's of million of dollars, accelerate construction, and improve the repository's performance. This development program

was designed to meet the economic and engineering properties of the appropriate cementitious materials to build out these tunnels<sup>1</sup>. This work supposes that cementitious liners and invert (the flat bedding placed in the drifts upon which the rails are laid) will be used ultimately in the second-generation repository design. This paper describes the required properties of YM-compatible cements and the program to

develop and test materials for a suite of underground construction technologies. Specifically, this paper addresses mitigation of potential impacts of free calcium hydroxide in the concrete and grout binding matrices. Part II describes the formulation and testing in detail.

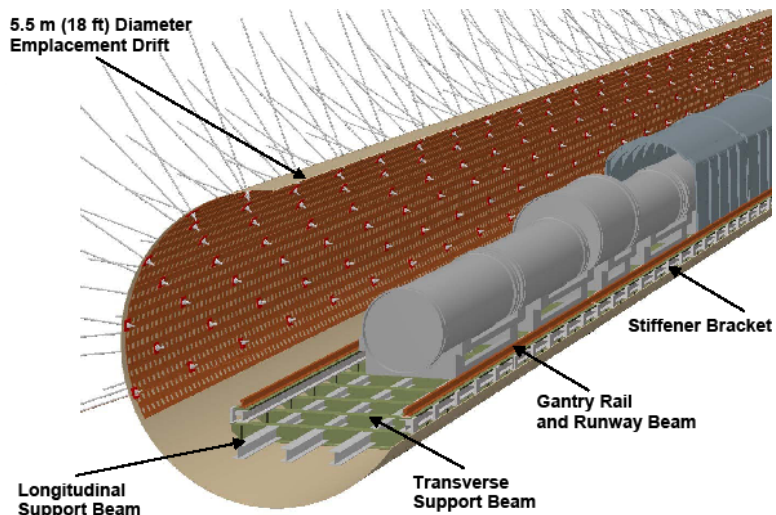


*Figure 1-1. Current YMP baseline underground tunnel build-out construction technology.*

## 1.2 Background

Based on several concerns described throughout the YMP document on the *Evaluation of Alternative Materials for Emplacement Drift Ground Control* (BCAA00000-01717-0200-00013 REV 00)<sup>2</sup>, the wide use of cements is currently not included in the YM repository construction plans.

Current safety-assessment models used by the YMP assume that (1) cements accelerate the release and increase the mobility of uranium, fission products, and actinides and (2) specific selected mechanisms apply to the formation and the behavior of uranium and radionuclides in concrete-modified groundwater. These assumptions resulted in the prediction of a dose rate increase of a 100-fold for the 10,000-year peak dose to the average member of the critical off-site group. The specific chemical reactions supporting these assumptions are based on previous experience in processing uranium ore; data for these reactions are then extrapolated to the geochemical conditions of the YM site.

### 1.3 Summary of YMP Concerns

The principal concerns with the use of ordinary Portland cement (OPC) in YMP are

1. Leachates from concrete with a high pH (>10) in contact with  $\text{UO}_2$  could increase radionuclide solubility and mobility.
2. Water from the dehydration of concretes could increase the relative humidity in the tunnels and drifts.
3. Leachates from cement could dissolve the adjacent vitreous tuff and could increase the porosity, permeability, and transport properties of the adjacent formation and could result in higher water-borne transport rates of nuclides.
4. Superplasticizers in the concrete matrix could form organic acids that stabilize colloids, thereby increasing radionuclide transport from the repository.
5. The organics and calcium sulfate hydrate (gypsum) could provide a substrate for microbiological growth that would accelerate corrosion of the waste package and increase the availability of radionuclides for transport to near and far field.
6. It is very difficult to show that engineered materials are durable in the time scales (10,000 to 1,000,000 years) of the YMP risk assessments.

*(Issues two through six are addressed in detail in reference 1.)*

The first of these assumptions is based on the potential impacts of soluble free calcium hydroxide (Portlandite) found in OPC and the carbonate YM groundwaters. The hexagonal crystals of Portlandite ( $\text{Ca}(\text{OH})_2$ ) are the most soluble, leachable phase that is embedded in the cured OPC matrix. If there were no additional buffering of the pH by a solution saturated in silicates, the hydroxyl ion,  $\text{OH}^-$ , concentrations could rise to above  $1 \times 10^{-4}$  mol/L (pH >10). In the presence of this high pH and groundwater carbonate anions ( $\text{CO}_3^{2-}$ ), formation of very soluble, mobile uranyl carbonate species, such as  $\text{UO}_2(\text{CO}_3)_2^{-2}$  and  $\text{UO}_2(\text{CO}_3)_3^{-4}$  can occur<sup>3</sup>. However, these soluble uranium products do not occur if the groundwater-leachate or cement porewaters are saturated in silicates and aluminates and are consequently buffered.

In the case of high-silica pozzolanic cement formulations, calcium hydroxide is consumed by reaction with glassy silica [ $\text{SiO}_2$  (G)] (equation 1):



$$\Delta G_{35^\circ\text{C}} = -9 \text{ kcal/mol}$$

In the cementitious binder, an excess  $\text{SiO}_2(\text{G})$  will eventually consume all of the free calcium hydroxide and buffer the leachates to below 10 pH. Originally, the YMP did not consider the beneficial reactions<sup>4</sup> that would occur in the presence of high-silica cements. With high-silica cements, the waste package (WP), uranium, and groundwater interactions actually retard the release and migration of radioactivity from the repository. With high-silica materials, the concrete-modified YM groundwater can significantly delay the release and retard the mobility of uranium, fission products, and actinides<sup>5,6</sup> by factors of 1/100 to 1/10,000.

## 1.4 Selection of Materials and Concrete and Grout Formulation

To develop cementitious liners and inverters that are compatible with the YM repository performance requirements, we first surveyed possible sources of cements, pozzolans, sands, and aggregates in the southeastern United States. We took some care to select suppliers that would likely still be in existence when construction of the YM repository would begin to use cementitious liners and inverters about years 2015 to 2025. The results of this search, selection, and testing are presented in Part II of this paper. We tested blends of type V Portland cement with a suite of additives, which had a range of particle sizes and silica reactivities. Some free calcium hydroxide is needed early in the curing stages to ensure adhesion between the paste and the fine quartz and coarse basalt aggregates. However, by the end of the initial curing of about 60 days, there should be no Portlandite crystals of free calcium hydroxide.

Based on experience with pozzolanic formulations, we also planned to avoid heat shrinkage and binder shrinkage by promoting the early formation of high-density calcium silicate hydrates (CSH), thus minimizing the internal stresses that lead to microcracking of the concretes and grouts. Also, to help minimize the impacts of paste-shrinkage, steel microreinforcement fibers were added to these formulations.

As described in Part II, a binder blend of 40% by weight type V Portland cement (V-OPC), 30% blast furnace slag (BFS), 25% fly ash (FA), and 5% silica fume (SF) was selected based on its free-calcium hydroxide balance over time and its rate of strength development. Clean feldspar containing a very large amount of silica and minor quantities of  $\text{Al}_2\text{O}_3$ ,  $\text{Na}_2\text{O}$ ,  $\text{K}_2\text{O}$  and  $\text{Fe}_2\text{O}_3$  was chosen from a reliable supplier. Unweathered black, crushed basalt from the western slope of the Rocky Mountains was chosen for its silica (53% by weight,  $\text{SiO}_2$ ) and iron (~13% by weight, as  $\text{Fe}_2\text{O}_3$ ) contents.

The coarse aggregate basalt was produced by Martin Marietta Aggregates in its Mountain Quarry in Oroville, California. This common igneous rock is very hard and is fine-grained due to rapid cooling of lava. This unweathered basalt is black, characterized by a preponderance of calcic plagioclase feldspars and pyroxene together with minor amounts of accessory minerals such as olivine.

Two formulations were developed: (1) a high-strength concrete for the tunnel inverts upon which the rails are placed and waste packages will be transported and stored and (2) grout designed to be applied by a shotcrete process. With the support of the former chairman of ACI Committee 506 (shotcrete), Peter Tatnall of Performance Concrete Technology (PCT), both formulations were confirmed to comply with American Society for Testing and Materials (ASTM) and the American Concrete Institute (ACI) guidelines for particle size grading.

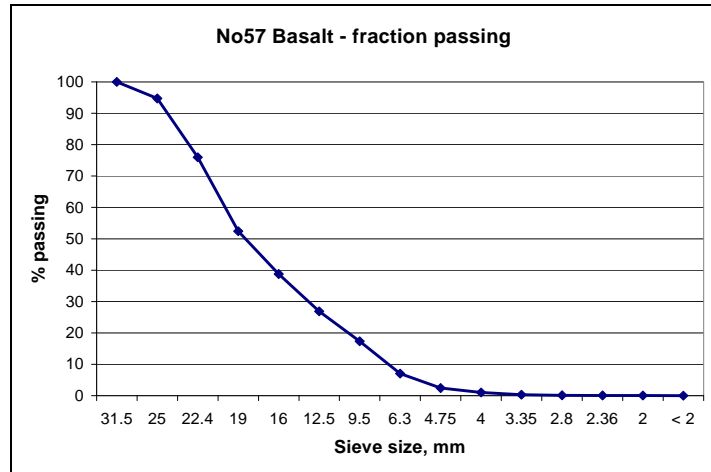


**Figure 1-2. Cumulative particle sizes, showing basalt aggregate's compliance with No. 57 ASTM C33-03 guidelines.**

For the inverts and shotcrete, the ASTM C33-03 standard's Table 2 provides the grading requirements for coarse aggregates. Two different aggregate sizes from the quarry: the size No. 57 (25.0 to 4.75 mm) is to be used for the invert concrete formulation, while the size No. 8 (9.5 to 2.36 mm) is used for the shotcrete formulation. The particle size analysis is presented in Figures 1-2 and 1-3 for both size ranges, ASTM C33 No. 57 and No.8. This No. 8 aggregate was also consistent with ASTM C1436-99 grade No. 2 for shotcrete.

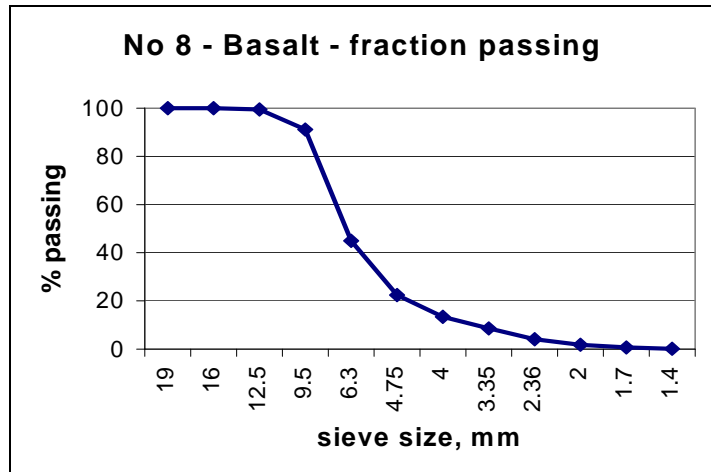


**Figure 1-3. Cumulative particle size, showing basalt aggregate's compliance of No.8 to ASTM C33-03 and No. 2 ASTM C1436-99 guidelines.**

A sample of the aggregate was digested using a combination of acids then analyzed by ICP–AES using a Thermo Jarrell Ash 61E Trace instrument. The chemical composition for the major constituents as well as the density result is found in Table 1-1.

From the steel microreinforcement, blast furnace slag, and basalt this concrete and grout has significant reducing capacity. The oxidation state of the system depends on the depth within the concrete, rates of heterogeneous reaction, and attainment of homogeneous equilibrium within the pore water. Where oxygen is depleted, the Eh would fall to around –300 mV even at pH = 12. With oxygen depletion, and residual pyrrhotite, Eh would remain at about -500 mV at pH = 12. This Eh measurement suggests that Fe<sup>2+</sup>/Fe<sup>3+</sup>, rather than S<sup>2-</sup>/SO<sub>4</sub><sup>2-</sup>, is controlling the redox state. However, the oxidation of sulfide involves the formation of many unstable

**Table 1-1. Analysis of the basalt aggregate**

Compound	% oxide		
Al <sub>2</sub> O <sub>3</sub>	11.7	±	0.9
CaO	7.2	±	0.7
as Fe <sub>2</sub> O <sub>3</sub>	12.8	±	0.9
K <sub>2</sub> O	1.7	±	0.2
MgO	3.6	±	0.3
Na <sub>2</sub> O	3.0	±	0.3
SiO <sub>2</sub>	53	±	5
TiO <sub>2</sub>	2.4	±	0.2
Density (g/cm <sup>3</sup> )	2.82		

intermediate oxidation states, such as sulfite and thionate, so the picture could be complicated by redox buffers of sulfur intermediate oxidation states. However, the basalt aggregate with about 10% by weight FeO has a far higher redox buffering capacity than an equivalent quantity of blast furnace slag<sup>7</sup>. This also indicates the reducing capacity of these formulations could still persist even without the silicate buffering to below 10 pH.

Table 1-2 lists U(VI) species that can form under these Eh and pH conditions in the aerobic YM repository with calcium-silica saturation<sup>4,8,9</sup>. For these major U(VI) species that have been observed, Table 1-2 also shows their Gibbs energies of formation, ΔG<sup>o</sup><sub>f</sub>, 298. In the case of reducing spent fuel dissolution after the waste packages fail, evidence shows a dense mat of alteration phases developed on the fuel surface, accompanied by depletion in the alkali and alkaline earth cations and Si in the leachate solution<sup>10</sup>. The nature of these alteration phases and the sequence in which they appear on the fuel are similar to those observed in surficial weathering zones of natural uraninite deposits<sup>11</sup>, with alkali and alkaline earth uranyl silicates being the long-term solubility limiting phases for uranium. The sequence observed is represented schematically in Figure 1-3. The formation of this layer of alteration (or corrosion) products retards releases of U.

**Table 1-2. Values of  $\Delta G_{f,298}^{\circ}$  for the U(VI) minerals**

Uranyl phases	Formula	kJoule/mol <sup>a</sup>	kJoule/mol <sup>b</sup>
Metaschoepite	$[(\text{UO}_2)_8\text{O}_2(\text{OH})_{12}] \cdot (\text{H}_2\text{O})_{10}$	-13,092.0	-13,092.0
Becquerelite	$\text{Ca}[(\text{UO}_2)_6\text{O}_4(\text{OH})_6] \cdot (\text{H}_2\text{O})_8$	-10,324.7	-10,305.8
Rutherfordine	$\text{UO}_2\text{CO}_3$	-1,563.0	-1,563.0
Uranocalcarite	$\text{Ca}_2[(\text{UO}_2)_3(\text{CO}_3)(\text{OH})_6] \cdot (\text{H}_2\text{O})_3$	-6,036.7	-6,037.0
Sharpite	$\text{Ca}[(\text{UO}_2)_6(\text{CO}_3)_5(\text{OH})_4] \cdot (\text{H}_2\text{O})_6$	-11,607.6	-11,601.1
Fontanite	$\text{Ca}[(\text{UO}_2)_3(\text{CO}_3)_4] \cdot (\text{H}_2\text{O})_3$	-6,524.7	-6,523.1
Liebigite	$\text{Ca}_2[(\text{UO}_2)(\text{CO}_3)_3] \cdot (\text{H}_2\text{O})_{11}$	-6,446.4	-6,468.6
Haiweeite	$\text{Ca}[(\text{UO}_2)_2(\text{Si}_2\text{O}_5)_3] \cdot (\text{H}_2\text{O})_5$	-9,367.2	-9,431.4
Ursilite	$\text{Ca}_4[(\text{UO}_2)_4(\text{Si}_2\text{O}_5)_5(\text{OH})_6] \cdot (\text{H}_2\text{O})_{15}$	-20,377.4	-20,504.6
Soddyite	$[(\text{UO}_2)_2 \text{SiO}_4] \cdot (\text{H}_2\text{O})_2$	-3,653.0	-3,658.0
Uranophane	$\text{Ca}[(\text{UO}_2)(\text{SiO}_3\text{OH})_2] \cdot (\text{H}_2\text{O})_5$	-6,192.3	-6,210.6

<sup>a</sup> Source: Chen, F.; R. C. Ewing; and S. B. Clark. 1999. "The Gibbs Free Energies and Enthalpies of  $\text{U}^{6+}$  Phases: An Empirical Method of Prediction." *American Mineralogist* **84**, pp 650–664.

<sup>b</sup> Source: Finch, R. J. 1997. "Thermodynamic Stabilities of U(VI) Minerals: Estimated and Observed Relationships, Scientific Basis for Nuclear Waste Management XX," Materials Research Society Proceedings, W.J. Gray and I.R. Triay, Eds., 465, pp. 1185–1192.

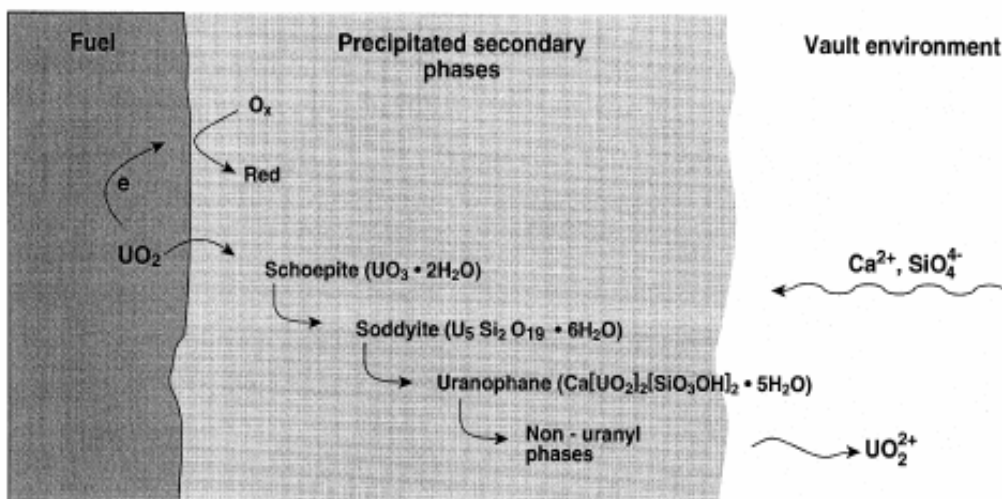


**Figure 1-3. Reaction sequence showing the alteration<sup>11</sup> of unirradiated  $\text{UO}_2$ .**

## 1.5 Conclusions

Using regional materials, we have successfully formulated a high-silica low pH binder with no free hydroxide after 60 days of curing for use in (1) a high-strength concrete for the tunnel invert upon which the rails are placed and waste packages will be transported and stored and (2) a pumpable concrete designed to be applied by a wet shotcrete process.

Preliminary testing shows that free calcium hydroxide is eliminated and that the rate of strength development is consistent with current engineering and application practices. The concrete inverts are expected to be manufactured by casting prestressed units on the surface to be delivered to the tunnels with the rails attached. The finer grained pumpable concrete for the tunnel liners will be applied by the wet shotcrete process immediately after excavation, using standard mine construction practices (Fig. 1-4). Compared with the current baseline design, these technologies may reduce the costs of the repository construction by as much as \$500M (USD).

After a year of accelerated, aggressive laboratory exposure tests, no adverse paste aggregate interaction has occurred under conditions bracketing the expected service environments. Testing continues to address the many issues concerning the long-term durability of these formulations in the YM repository.

Funding permitting, it is intended that a series of pilot-scale tests should be performed in order to finish the shotcrete formulation, which will require addition of a set-accelerator and an adjustment of the final water content.

All results so far show that these formulations are compatible with current engineering practices and are expected to be integrated into the second generation of YMP repository design and construction.

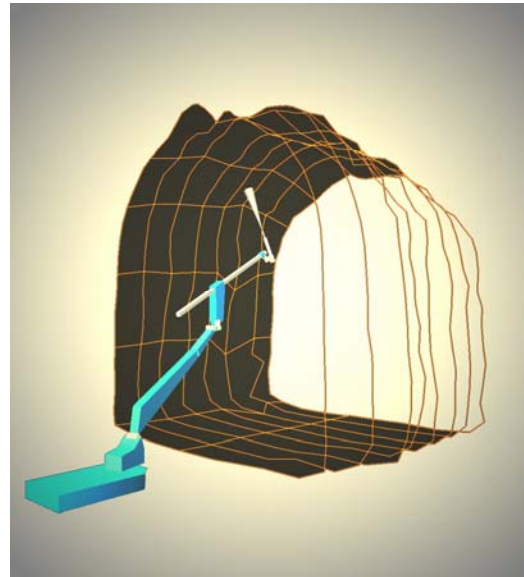


***Figure 1- 4. Computer-controlled spraying robot that scans an area with a laser, uses a single joystick, and is able to work manually or fully automatic.***

## References

- 1 **Dole, L.R., C.H. Mattus, M. Fayek, L.M. Anovitz, J.J. Ferrada, D.J. Wesolowski, D. Olander, D.A. Palmer, L.R. Riciputi, L. Delmau, S. Ermichev and V.I. Shapovalov. 2004.** “Cost-Effective Cementitious Material Compatible with Yucca Mountain Repository Geochemistry.” ORNL/TM-2004/296, Oak Ridge National Laboratory, UT-Battelle, LLC, Oak Ridge, TN.
- 2 **BCAA00000-01717-0200-00013 REV 00**, Sections 6.2.1- 6.2.2, “Evaluation of Alternative Materials for Emplacement Drift Ground Control, pp. 7-8 (referring to greater peak 10,000 year doses, Table 6-1).
- 3 **Langmuir, D. 1978.** “Uranium Solution-Mineral Equilibrium at Low Temperatures with Applications to Sedimentary Ore Deposits.” *Geochimica et Cosmochimica Acta* **42**(6), pp. 547–569.
- 4 **Finch, R. J. 1997.** “Thermodynamic Stabilities of U(VI) Minerals: Estimated and Observed Relationships, Scientific Basis for Nuclear Waste Management XX,” Materials Research Society Proceedings, W.J. Gray and I.R. Triay , Eds., 465, pp. 1185–1192.
- 5 **Mattus, C. H. and L. R. Dole. 2003.** “Durability of Depleted Uranium Aggregates (DUAGG) in DUCRETE Shielding Applications,” International High-Level Radioactive Waste Management Conference, Las Vegas, NV, USA, American Nuclear Society, La Grange Park, IL USA, 03/30/2003–04/02/2003.
- 6 **Glasser F. P. 1993.** Chemistry of Cement-Solidified Waste Forms, in Chemistry and Microstructure of Solidified Waste Forms. Edited by R. D. Spence, Oak Ridge National Laboratory, Lewis Publishers.
- 7 **John Apps. 2006.** Correspondence with John Apps of Lawrence Berkeley National Laboratory, August 24, 2006.
- 8 **Chen, F., R. C., Ewing, and S. B., Clark. 1999.** “The Gibbs Free Energies and Enthalpies of U6+ Phases: An Empirical Method of Prediction.” *American Mineralogist* **84**, pp 650–664.
- 9 **Freeze, R. A. and A. J. Cherry. 1979.** *Groundwater*. Prentice-Hall, Inc., Englewood Cliffs, New Jersey, pp. 254–289.
- 10 **Shoesmith, D. W. 2000.** “Fuel Corrosion Processes Under Waste Disposal Conditions,” *Journal of Nuclear Materials*, 282, pp. 1–31.
- 11 **Wronkiewicz, D.J.; J. K. Bates, S. F. Wolf, and E.C. Buck. 1996.** “Ten-year results from unsaturated drip tests with UO<sub>2</sub> at 90°C: implications for the corrosion of spent nuclear fuel,” *Journal of Nuclear Materials*, **238**, 78.